

Supporting Information

How stereochemistry of lipid components can affect lipid organization and the route of liposome internalization into cells

Stefano Borocci,^{1,2*} Giuseppina Bozzuto,³ Cecilia Bombelli,⁴ Francesca Ceccacci,⁴ Giuseppe Formisano,³ Annarita Stringaro,³ Agnese Molinari,^{3*} Giovanna Mancini^{2*}

Affiliations:

¹Dipartimento per la Innovazione nei sistemi Biologici, Agroalimentari e Forestali (DIBAF), Università degli Studi della Tuscia, L.go dell'Università, s.n.c., 01100 Viterbo, Italy

CNR, Istituto per i Sistemi Biologici, Area della Ricerca di Roma 1, via Salaria Km 29,300, 00015 Monterotondo (Roma), Italy.

³Centro Nazionale per la Ricerca e la Valutazione preclinica e clinica dei Farmaci, Istituto Superiore di Sanità, Viale Regina Elena 299, 00161 Roma, Italy.

⁴CNR, Istituto per i Sistemi Biologici, Sede Secondaria di Roma- Meccanismi di Reazione c/o Dipartimento di Chimica Università degli Studi di Roma "Sapienza", P.le A. Moro 5, 00185 Roma, Italy.

*Correspondence to giovanna.mancini@cnr.it; agnese.molinari@iss.it.

Table S1: Atom type and partial atomic charges used to describe gemini headgroups with the Berger Force Field.

n	Name	Atom type	Atomic Charge
1,2	CH ₃	LC3	0.219
3	CH ₂	LP2	0.219
4	N	LNL	0.124
5	CH ₂	LH2	0.219
6	CH	LH1	0.059
7	O	LOS	-0.414
8	CH ₃	LC3	0.355

Torsional parameter of O-CH₂-CH₂-O and CH₃-O-CH₂-CH₂

Torsional potential of O-C-C-O and C-O-C-C dihedral angles was determined by performing geometry optimization of dimethoxyethane (DME). The quantum mechanical energy was calculated at CCSD(T)/cc-pVTZ level of theory on the MP2/cc-pVDZ geometry of DME. At each step, the remaining internal degree of freedom were allowed to relax during the energy minimization. The molecular mechanics dihedral potential was built to include the nonbonded 1-4 interaction.

The torsional potential energy was described by using the Ryckaert-Bellemans dihedral potential:

$$V_{RB}(\phi_{ijkl}) = \sum_{n=0}^5 C_n (\cos(\phi - 180))^n$$

The Ryckaert-Bellemans coefficient, C_n , were obtained by minimizing the differences between the quantum mechanical and molecular mechanics potential energies and the corresponding Ryckaert-Bellemans potential values.

Table S2: Torsional Parameter (in units of kJ mol⁻¹) for the O-CH₂-CH₂-O, CH₃-O-CH₂-CH₂ dihedral of DME

Torsional Angle	C ₀	C ₁	C ₂	C ₃	C ₄	C ₅
O-CH ₂ -CH ₂ -O	1.6539	20.2169	6.014	-32.127	2.3622	1.7444
CH ₃ -O-CH ₂ -CH ₂	3.0131	11.6689	1.0591	-11.9327	-0.2041	-3.7430

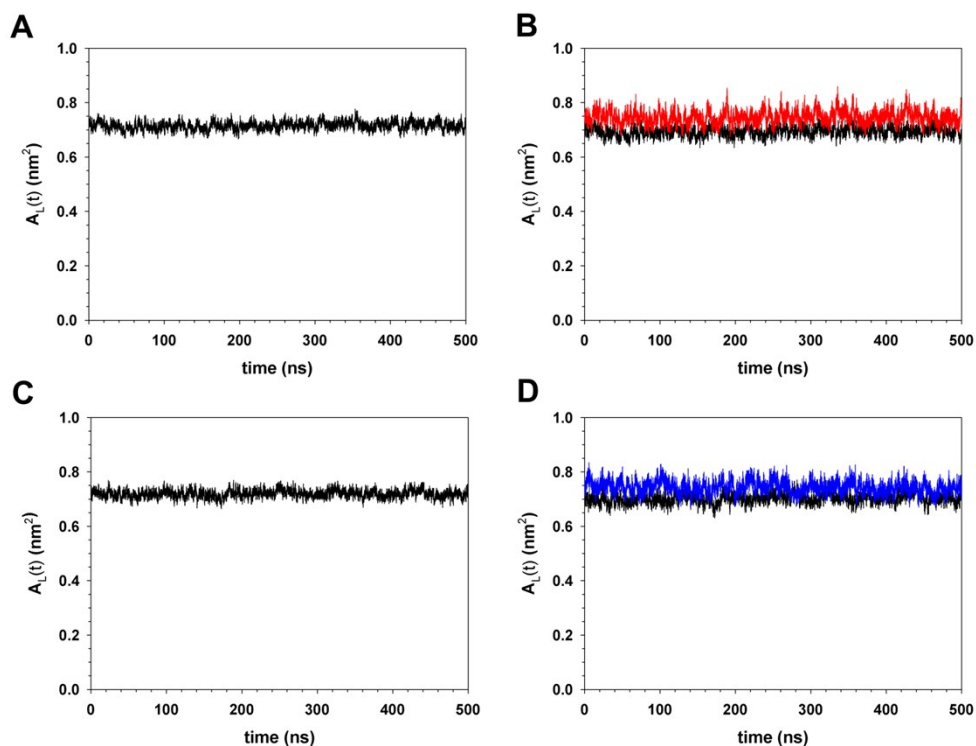


Figure S1: Time evolution at 310 K of the area per lipid, $A_L(t)$, calculated by dividing the lateral (XY) dimensions of the simulated box of DMPC/1a (A) and DMPC/1b (C). Time evolution of the area per lipid, $A_L(t)$, calculated by Voronoi tessellation of DMPC/1a (B) (DMPC black line and 1a red line) and DMPC/1b (D) (DMPC black line and 1b red line).

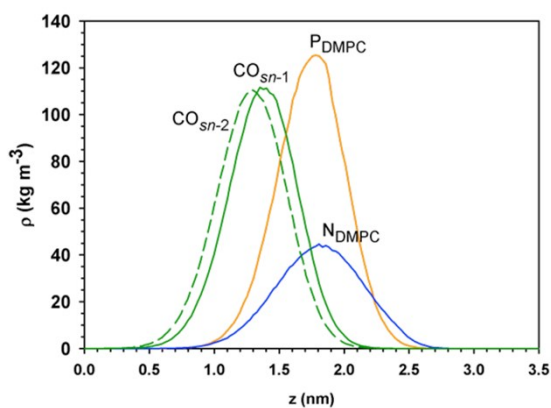


Figure S2: Mass density profiles of selected atoms of DMPC across lipid bilayer. The mass density is calculated with respect to the lipid bilayer center ($z = 0$).

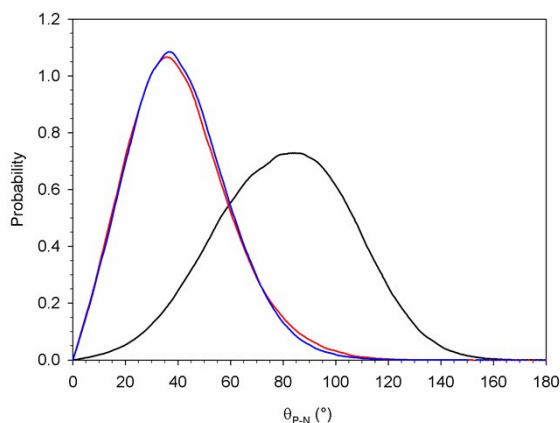


Figure S3: Orientation of P-N vector with respect to the normal bilayer of pure DMPC (black line), DMPC/**1a** (red line) and DMPC/**1b** (blue line).

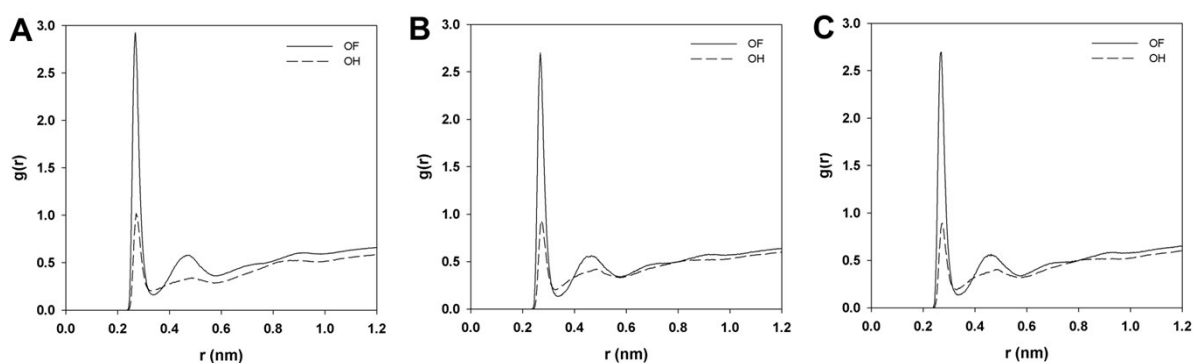


Figure S4: Radial distribution function of water around non-ester oxygen atoms OF and OH of DMPC in DMPC (**A**) in DMPC/**1a** (**B**) and DMPC/**1b** (**C**) bilayers.

Lateral Diffusion of Water.

The calculation of the lateral diffusion coefficients of water (D_{lat} - parallel to lipid bilayer surface) allow us to evaluate the translational mobility of water close to lipid bilayer. Figure S5 reports the values of lateral diffusion coefficients (D_{lat}) of water molecules calculated as a function of the distance d from the surface of lipid bilayer by dividing the d dimension into 0.2 nm slabs.

The lateral diffusion coefficient D_{lat} of water molecules, associated with the different slabs close to the bilayer surface, was calculated from the mean square displacement (MSD) of water molecules using the Einstein equation:

$$D_{lat} = \lim_{t \rightarrow \infty} \frac{\langle |\vec{r}(t)| - |\vec{r}(t_0)|^2 \rangle}{4t}$$

The MSD of water in each slab was calculated over 20 ps intervals by considering only the water molecules located in same zone at time t_0 and t .

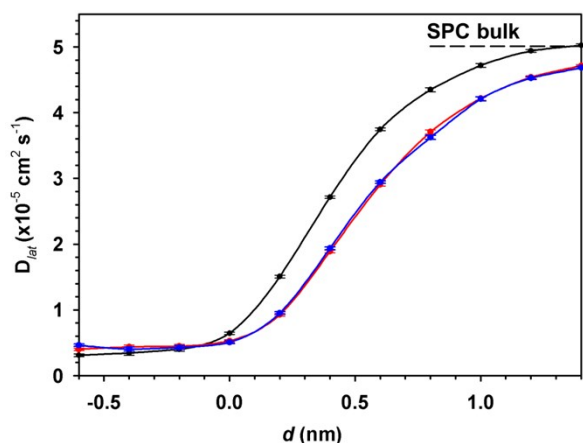


Figure S5. The lateral diffusion coefficient (D_{lat}) of water molecules as a function of distance d from the membrane-water interface of DMPC (black line), DMPC/**1a** (red line) and DMPC/**1b** (blue line).

For all simulated systems, water mobility increases as a function of the distance from the lipid/water interface, due to the decrease of interaction between water molecules and lipids, in agreement with literature data^{S1,S2,S3}. In the case of DMPC bilayer we obtained a value of lateral diffusion for the bulk water molecules of $(5.01 \pm 0.02) \times 10^{-5} \text{ cm}^2 \text{ s}^{-1}$ in agreement with literature data².

In the case of DMPC/1 the water mobility is reduced with respect to mere DMPC and not influenced by the nature of gemini component. The lateral diffusion of water at the membrane-water interface of DMPC/1 is influenced by the nature of interaction between water molecules and lipid/gemini

components and also by the presence of chloride ions that neutralise the positive charges of gemini. The chloride ions, localised mainly in the region II and III (Figure 3), due to high mass, slow down the diffusion of water molecules with respect to water molecules at the membrane-water interface of DMPC.

References

- S1. S. Y. Bhide and M. L. Berkowitz, *J. Chem. Phys.* 2005, **123**, 224702.
- S2. S. W. I. Siu, R. Vácha, P. Jungwirth and R. A. Böckmann, *J. Chem. Phys.* 2008, **128**, 125103.
- S3. J. Yang, C. Calero and J. Martí, *J. Chem. Phys.* 2014, **140**, 104901.